Hybrid Materials Containing Metal(II) Schiff Base Complex Covalently Linked to the Silica Matrix by Two Si−C Bonds: Reaction with Dioxygen

Robert J. P. Corriu,[†] Emmanuelle Lancelle-Beltran,[†] Ahmad Mehdi,[†] Catherine Reyé,*[,†] Stéphane Brandès,[‡] and Roger Guilard[‡]

Laboratoire de Chimie Moléculaire et Organisation du Solide, UMR 5637 CNRS, Université de Montpellier II, Sciences et Techniques du Languedoc, Place E. Bataillon, F-34095 Montpellier Cedex 5, France, and Laboratoire d'Ingénierie Moléculaire pour la Séparation et les Applications des Gaz, LIMSAG, UMR 5633, Université de Bourgogne, 6, Boulevard Gabriel, 21100 Dijon, France

Received February 20, 2003. Revised Manuscript Received May 21, 2003

A bis-silylated pentadentate Schiff base formed from substituted salicylaldehyde and bis-(3-aminopropyl)amine has been prepared and isolated to give rise via the sol−gel process to hybrid materials containing metal Schiff base complexes covalently bonded to the silica matrix. For that purpose, two routes of complexation have been investigated: the first corresponds to the hydrolysis and polycondensation of the bis-silylated metal Schiff base complex (route A) and the second to the hydrolysis and polycondensation of the bis-silylated Schiff base followed by the complexation of organic moieties immobilized on silica (route B). We have shown that the geometry of metal Schiff base complexes immobilized on silica is a function on the route of preparation of materials. Furthermore, the study of the O_2-binding capacity of these materials revealed that only the hybrid materials prepared under well-controlled experimental conditions via route A are able to bind notably dioxygen, showing thus the versatility of the sol−gel approach.

Introduction

Oxygen adducts of transition metal complexes have attracted interest owing to their roles in biological processes[1,2] and catalysis.[3−6] A large number of complexes containing Fe^{II}, Co^{II}, Mn^{II}, or Cu^{I} are known to undergo reversible coordination of the dioxygen ligand in solution.[7,8] However, dioxygen carriers in solution usually suffer from the problem of oxidative degradations to form inert complexes, reactions which increase with the concentration.[9] Incorporation of dioxygen-reactive complexes within the matrixes of polymers constitutes one of the strategies that were developed to inhibit these processes.[10−15] Indeed, the heterogenization of reagents presents the engineering advantages of heterogeneous catalysts, that is, ease of handling, simplification of methods for recycling, low toxicity, and no use of solvents.

Among the various kinds of solid supports, silica matrix was considered for the immobilization of catalytic complexes such as Schiff base derivatives.[16−19] We have used[20] this strategy for the immobilization of cobalt(II) bis(salicylaldehyde)ethylenediamine (Co-salen) and cobalt(II) bis(3-fluorosalicylaldehyde)ethylenediamine (Co-fluomine), which are the most extensively studied among the oxygen-binding cobalt complexes.[21−23] Our

* To whom correspondence should be addressed. E-mail: reye@univ-montp2.fr.
[†] Université de Montpellier II.
[‡] Université de Bourgogne.

(1) Sykes, A. G. In *Advanced Inorganic Bioinorganic Mech.*; Sykes, A. G., Ed.; Academic Press: New York, 1982; pp 121−178.
(2) Jameson, G. B.; Ibers, J. A. In *Bioinorganic Chemistry*; Bertini, I., Gray, H. B., Lippard, S. J., Valentine, J. S., Eds.; Univ Science Books: Hill Valley, CA, 1994; pp 167−252.
(3) Wöhrle, D.; Bohlen, H.; Aringer, C.; Pohl, D. *Makromol. Chem.* **1984**, *185*, 669−685.
(4) Bailey, C. L.; Drago, R. S. *Coord. Chem. Rev.* **1987**, *79*, 321−332.
(5) Frunza, L.; Kosslick, H.; Landmesser, H.; Höft, E.; Fricke, R. *J. Mol. Catal. A: Chem.* **1997**, *123*, 179−187.
(6) Solomon, E. I.; Sundaram, U. M.; Machonkin, T. E. *Chem. Rev.* **1996**, *96*, 2563−2605.
(7) Jones, D. R.; Summerville, D. A.; Basolo, F. *Chem. Rev.* **1979**, *79*, 139−179.
(8) Niederhoffer, E. C.; Timmons, J. H.; Martell, A. E. *Chem. Rev.* **1984**, *84*, 137−203.
(9) Martell, A. E. *Oxygen Complexes and Oxygen Activation by Transition Metals*; Martell, A. E., Sawyer, D. T., Eds.; Plenum: New York, 1988.
(10) Collman, J. P.; Reed, C. A. *J. Am. Chem. Soc.* **1973**, *95*, 2048−2049.
(11) Fuhrhop, J. H.; Beseke, S.; Vogt, W.; Ernst, J.; Subramanian, J. *Makromol. Chem.* **1977**, *178*, 1621−1631.
(12) Nishide, H.; Tsukahara, Y.; Tsuchida, E. *J. Phys. Chem. B* **1998**, *102*, 8766−8770.
(13) Nishide, H.; Mizuma, H.; Tsuchida, E.; McBreen, J. *Bull. Chem. Soc. Jpn.* **1999**, *72*, 1123−1127.
(14) Yang, J.; Huang, P. *Chem. Mater.* **2000**, *12*, 2693−2697.
(15) Sharma, A. C.; Borovik, A. S. *J. Am. Chem. Soc.* **2000**, *122*, 8946−8955.
(16) Sutra, P.; Brunel, D. *Chem. Commun.* **1996**, 2485−2486.
(17) Chisem, I. C.; Rafelt, J.; Shieh, M. T.; Chisem, J.; Clark, J. H.; Jachuck, R.; Macquarrie, D.; Ramshaw, C.; Scott, K. *Chem. Commun.* **1998**, 1949−1950.
(18) Zhou, X.-G.; Yu, X.-Q.; Huang, J.-S.; Li, S.-G.; Li, L.-S.; Che, C.-M. *Chem. Commun.* **1999**, 1789−1790.
(19) Brunel, D. *Microporous Mesoporous Mater.* **1999**, *27*, 329−344.
(20) Corriu, R. J. P.; Lancelle-Beltran, E.; Mehdi, A.; Reyé, C.; Brandès, S.; Guilard, R. *J. Mater. Chem.* **2002**, *12*, 1355−1362.
(21) Calvin, M.; Martell, A. E. *Chemistry of the Metal Chelate Compounds*; Prentice Hall: New York, 1952.
(22) Li, G. Q.; Govind, R. *Ind. Eng. Chem. Res.* **1994**, *33*, 755−783.

10.1021/cm0302330 CCC: $25.00
Published on Web 07/04/2003

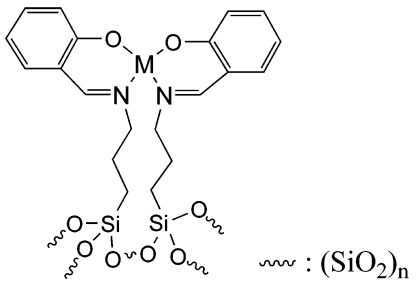

Figure 1. Immobilization of silyl ether-modified salen in a silica gel.

approach implied two steps: the first was the preparation of ordered mesoporous silica functionalized with a ligand able to coordinate the metal Schiff base complexes. The second was the binding via a coordination bond formation of the metal Schiff base complexes into the ordered mesoporous functionalized silica. However, the attachment of the metal Schiff base complexes via a coordinative bond can give rise to their leaching. Therefore, in a continuation of our study on nanostructured hybrid materials,[24,25] we decided to immobilize metal Schiff base complexes on silica matrix via two covalent bonds with the aim to prepare materials with oxygen binding ability. The presence of two hydrolyzable $Si(OR)_3$ groups on the Schiff base complexes allows the preparation of hybrid materials without dilution of the organic moieties into silica. For that purpose, a pentadentate Schiff base formed from a substituted salicylaldehyde and bis(3-aminopropyl)amine was chosen as the candidate. To the best of our knowledge, only one example of metal Schiff base complex immobilized on silica by two Si−C bonds was reported, with the view to prepare heterogeneous oxidation catalysts (Figure 1).[26]

In this paper, we describe the preparation of the isolated bis-silylated Schiff base **1** as well as the corresponding metal Schiff base complexes. Hybrid materials containing metal Schiff base complexes covalently bonded to the silica matrix were obtained via the sol−gel process following two different routes. The first one corresponds to the hydrolysis and polycondensation of the bis-silylated metal Schiff base complexes (Scheme 1, route A) and the second one to the hydrolysis and polycondensation of the bis-silylated Schiff base followed by the complexation of organic moieties immobilized on silica (Scheme 1, route B). We have shown that the geometry of the metal Schiff base complexes immobilized on silica is connected with the route of preparation of materials. Furthermore, the study of the O_2-binding capacity of these materials revealed that only the hybrid materials prepared under well-controlled experimental conditions following route A are able to bind notably dioxygen, showing thus the versatility of the sol−gel approach.

Experimental Section

All experiments were carried out with standard high-vacuum and Schlenk techniques. Solvents were dried and distilled just before use. *p*-(Chloromethyl)phenyltrichlorosilane was purchased from Avocado and 2,4-dihydroxybenzaldehyde and 3,3′-diaminodipropylamine from Acros organics. IR data were obtained on a Perkin-Elmer 1600 FTIR spectrophotometer. The melting points (mp) were measured with a Buchi B-540 apparatus and are uncorrected. The solution NMR spectra were recorded on a Bruker AC-200 (^{29}Si) and Bruker DPX-200 (^{1}H and ^{13}C). Chemical shifts (δ, ppm) were referenced to Me_4Si (^{1}H, ^{13}C, ^{29}Si). The abbreviations used are s for singlet, d for doublet, dd for double doublet, t for triplet, q for quartet, sept for septet, and m for multiplet. The CP MAS ^{29}Si solid-state NMR spectra were recorded on a Bruker FTAM 300 as well as CP MAS ^{13}C solid-state NMR spectra, in the latter case by using the TOSS technique. In both cases, the repetition time was 5 and 10 s with contact times of 5 and 2 ms. The EPR spectra were recorded in the solid state on a Bruker ESP 300 spectrometer at the X-band (9.6 GHz), from the "Centre de Spectrométrie Moléculaire de l'Université de Bourgogne", equipped with a double cavity and a liquid nitrogen cooling accessory. The EPR spectra were referenced to 2,2-diphenyl-1-picrylhydrazyl (DPPH) ($g = 2.0036$). Sensitive dioxygen compounds were transferred in the EPR tube in a glovebox under argon. FAB mass spectra [matrix, *m*-nitrobenzyl alcohol (NBA)] were recorded on a JEOL JMS-D3000 spectrometer. The UV−visible diffuse reflectance spectra (Kubelka−Munk units) were measured with a Perkin-Elmer Lambda 14 spectrophotometer equipped with a reflectance attachment. The reference used was MgO, and the xerogels were dispersed in MgO (3 wt %). Specific surface areas were determined by the Brunauer−Emmett−Teller (BET) method on a Micromeritics Gemini III 2375 analyzer, and the average pore diameters were calculated by the BJH method.[27] Elemental analyses were carried out by the "Service Central de Micro-Analyse du CNRS, Lyon".

Synthesis of Precursors. *Preparation of p-(Chloromethyl)-phenyltriisopropoxysilane.* To a mixture of distilled 2-propanol (22 mL) and anhydrous triethylamine (40 mL) in 120 mL of dried ether, in a three-necked flask equipped with a mechanical stirrer, a condenser, and an additional funnel, was added dropwise at 0 °C a solution of *p*-(chloromethyl)phenyltrichlorosilane (12.44 g, 0.048 mol) in ether (40 mL). A white precipitate was formed. The reaction mixture was stirred at room temperature for 2 h. The solvent was removed and the resulting white residue was stirred in pentane (400 mL). After filtration and concentration of the filtrate, the yellow residual liquid was distilled to afford 11.4 g of *p*-(chloromethyl)-phenyltriisopropoxysilane (0.034 mol, 72%) as a colorless liquid. bp 132 °C at 0.05 Torr. ^{1}H NMR (δ, 200 MHz, $CDCl_3$): 1.25 (18H, d, $^3J_{HH} = 6.1$ Hz, $OCH(CH_3)_2$), 4.31 (3H, sept, $^3J_{HH} = 6.1$ Hz, $OCH(CH_3)_2$), 4.62 (2H, s, CH_2Cl), 7.42 ($2H_{arom}$, dd, $^3J_{HH} = 6.4$ Hz, $^5J_{HH} = 1.8$ Hz), 7.72 ($2H_{arom}$, dd, $^3J_{HH} = 6.4$ Hz, $^5J_{HH} = 1.8$ Hz). ^{13}C NMR (δ, 50 MHz, $CDCl_3$): 25.94 ($OCH(CH_3)_2$), 46.38 (CH_2Cl), 65.86 ($OCH(CH_3)_2$), 128.17−139.53 (C_{arom}). ^{29}Si NMR (δ, 40 MHz, $CDCl_3$): −62.23. Anal. Calcd for $C_{16}H_{27}O_3SiCl$: C, 58.07; H, 8.22; Si, 8.49; Cl, 10.71. Found: C, 57.85; H, 8.18; Si, 8.55; Cl, 10.74.

*Preparation of [o-Hydroxy, p-(p-(oxomethylphenyl)triisopropoxysilyl)]benzaldehyde (**2**).* A mixture of 2,4-dihydroxybenzaldehyde (1.38 g, 10 mmol), dried $NaHCO_3$ (0.96 g, 11.4 mmol), dried KI (0.17 g, 1 mmol), 1.20 g of molecular sieve (3 Å), and anhydrous CH_3CN (20 mL) was placed in a Schlenk flask equipped with a condenser and heated to 60 °C. *p*-(Chloromethyl)phenyltriisopropoxysilane (4.30 g, 13 mmol) was then added over 1 min and the reaction mixture was stirred and heated under reflux for 6 h. The solvent was removed in vacuo and the residue dissolved in CH_2Cl_2. After filtration under argon, the filtrate was concentrated. The residual yellow oil was chromatographed over 180 g of silica gel. After elution with CH_2Cl_2 and removal of the solvent, 1.95 g (45%) of **2** as a yellow liquid was obtained. ^{1}H NMR (δ, 200 MHz, $CDCl_3$): 1.24 (18H, d, $^3J_{HH} = 6.1$ Hz, $OCH(CH_3)_2$), 4.31 (3H, sept., $^3J_{HH}$

(23) Hutson, N. D.; Yang, R. T. *Ind. Eng. Chem. Res.* **2000**, *39*, 2252−2259.
(24) Corriu, R. J. P. *Angew. Chem., Int. Ed.* **2000**, *39*, 1376−1398.
(25) Corriu, R. J. P. *Eur. J. Inorg. Chem.* **2001**, 1109−1121.
(26) Murphy, E. F.; Schmid, L.; Bürgi, T.; Maciejewski, M.; Baiker, A.; Günther, D.; Schneider, M. *Chem. Mater.* **2001**, *13*, 1296−1304.
(27) Barrett, E.; Joyner, L. G.; Halenda, P. P. *J. Am. Chem. Soc.* **1951**, *73*, 373−380.

Scheme 1

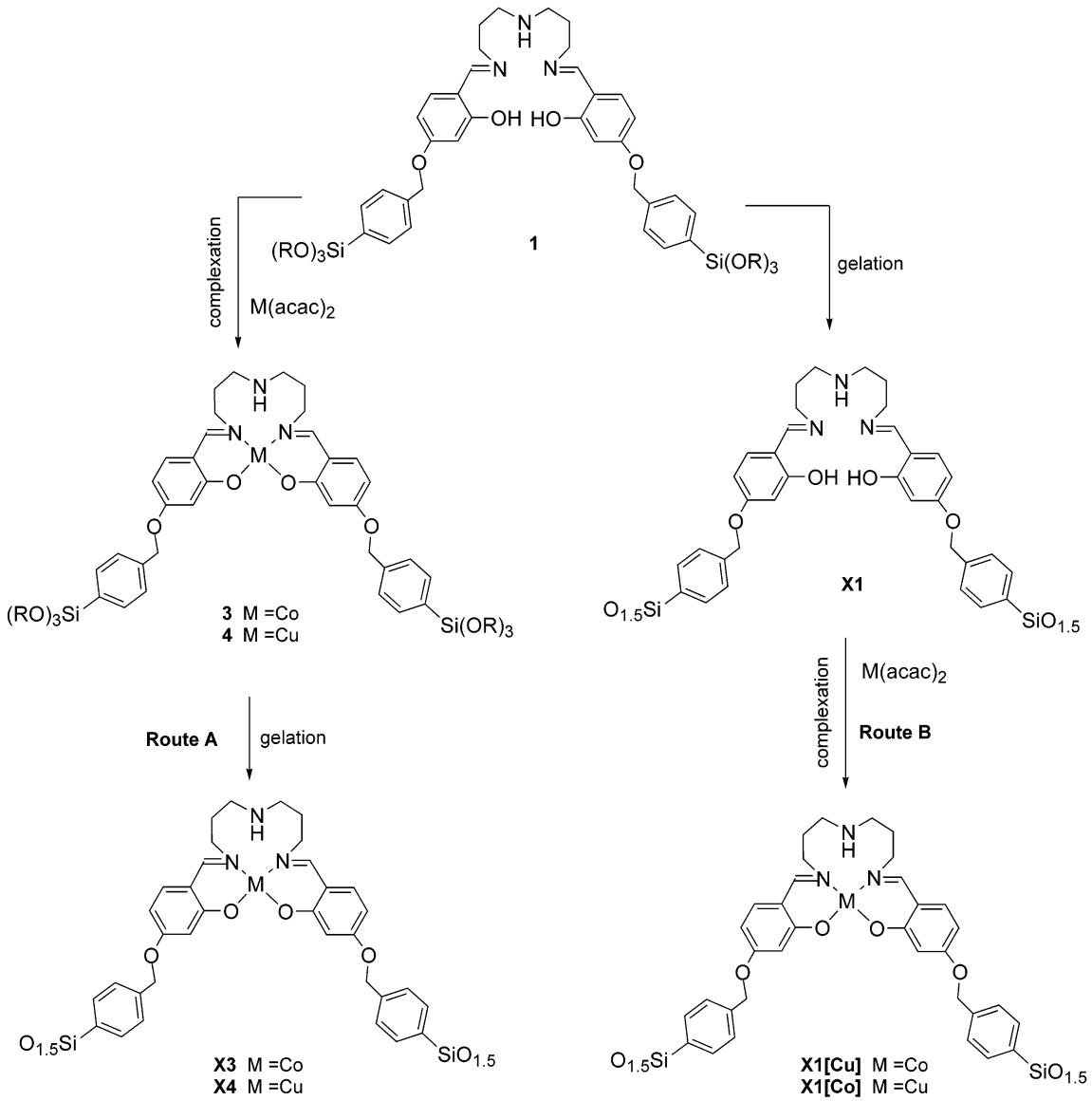

= 6.1 Hz, OC*H*(CH_3)$_2$), 5.15 (2H, s, CH_2O), 6.54−6.65 (2H$_{arom}$, m), 7.42−7.78 (4H$_{arom}$, dd, $^3J_{HH}$ = 8.6 Hz; 1H$_{arom}$, d, $^4J_{HH}$ = 8.1 Hz), 9.75 (C*H*O, s); 11.51 (O*H*, s).^{13}C NMR (δ, 50 MHz, $CDCl_3$): 25.94 (OCH(*C*H_3)$_2$), 65.85 (O*C*H(CH_3)$_2$), 70.54 (O*C*H_2), 102.00−109.10−115.74−127.03−133.62−135.65−135.68−137.90−164.79 and 166.15 (C_{arom}), 194.17 (H*C*=O). ^{29}Si NMR (δ, 40 MHz, $CDCl_3$): −62.12. MS (FAB+, NBA): *m*/*z* = 433 ((M+H)$^+$, 15), 295 ((O*i*Pr)$_3$SiPhCH_2^+, 20), 205 ((Si(O*i*Pr)$_3$)$^+$, 5). IR (cm^{-1}, oil): 1660 (ν C=O); 1643−1627−1572 (ν C=C); 1038 (ν Si−O). Anal. Calcd for $C_{23}H_{32}O_6Si$: C, 63.86; H, 7.46; Si, 6.49. Found: C, 63.94; H, 7.44; Si, 6.47.

Preparation of ***1***. 3,3′-Diaminodipropylamine (300 μL, 2.08 mmol) was added dropwise at room temperature to a solution of **2** (1.80 g, 4.16 mmol) in toluene (30 mL) containing molecular sieve (3 Å, 1 g). The solution became instantly yellow and was heated under reflux for 40 min. After evaporation of the solvent, the residual oil was dissolved in pentane (50 mL). After filtration and concentration of the filtrate, 1.96 g (98%) of **1** as a yellow oil was obtained. ^{1}H NMR (δ, 200 MHz, $CDCl_3$): 1.24 (36H, d, $^3J_{HH}$ = 6.1 Hz, OCH(CH_3)$_2$), 1.89 (5H, m, CH_2CH$_2$NH + N*H*), 2.75 (4H, m, CH_2NH), 3.64 (4H, m, CH=NCH_2), 4.30 (6H, sept, $^3J_{HH}$ = 6.1 Hz, OC*H*(CH_3)$_2$), 5.10 (4H, s, CH_2O), 6.43−7.76 (14H$_{arom}$ + 2OH, m), 8.17 (2H, s, C*H*=N). ^{13}C NMR (δ, 50 MHz, $CDCl_3$): 25.92 (OCH(*C*H_3)$_2$), 31.51 (CH$_2$−*C*H$_2$−CH$_2$), 47.82 (NH−*C*H$_2$), 55.73 (=N−*C*H$_2$), 65.84 (O*C*H(CH_3)$_2$), 70.25 (O*C*H_2), 102.83−107.27−112.70−127.00−133.06−135.62−138.60−163.36 and 167.22 (C_{arom}), 164.13 (H*C*=N). ^{29}Si NMR (δ, 40 MHz, $CDCl_3$): −61.68. MS (FAB+, NBA): *m*/*z* = 961 ((M+H)$^+$, 7), 295 ((O*i*Pr)$_3$SiPhCH_2^+, 3), 205 (Si(O*i*Pr)$_3^+$, 7). IR (KBr, cm^{-1}): 1627 (ν C=N), 1583−1463 (ν C=C), 1044 (ν Si−O). Anal. Calcd for $C_{52}H_{77}O_{10}N_3Si_2$: C, 65.03; H, 8.08; N, 4.38; Si, 5.85. Found: C, 64.89; H, 8.13; N, 4.46; Si, 5.95.

Preparation of ***3***. A purple solution of cobalt acetylacetonate (700 mg, 2.72 mmol) in 2-propanol (60 mL) was added under argon to a yellow solution of **1** (2.61 g, 2.72 mmol) in 2-propanol (40 mL). The solution became instantly brown and was heated under reflux for 3 h. After evaporation of the solvent, the solid was washed with pentane (20 mL) and then dried under vacuum to give 2.63 g of **3** as a brown powder in 95% yield. mp 162−163 °C (decomposition). MS (FAB+, NBA): *m*/*z* = 1017 ((M + H$^+$), 13), 721 (M−CH_2PhSi(O*i*Pr)$_3$ + H)$^+$, 2). IR (cm^{-1}, KBr): 1627 (ν C=N), 1600−1463 (ν C=C), 1038 (ν Si−O). Anal. Calcd for $C_{52}H_{75}N_3O_{10}Si_2Co$: C, 61.40; H, 7.43; N, 4.13; Si, 5.52; Co, 5.79. Found: C, 60.30; H, 7.58; N, 4.03; Si, 6.25; Co, 5.55.

Preparation of ***4***. A hot blue solution of copper acetylacetonate (1.06 g, 4.04 mmol) in 2-propanol (80 mL) was added under argon to a yellow solution of **1** (3.88 g, 4.04 mmol) in 2-propanol (60 mL). The green reaction solution was heated under reflux for 5 h. After removal of the solvent, the solid was washed with pentane (20 mL) and dried under vacuum. Recrystallization from dibutyl ether under argon yielded to **4** as a green powder in 82% yield. mp 179−180 °C (decomposi-

Scheme 2

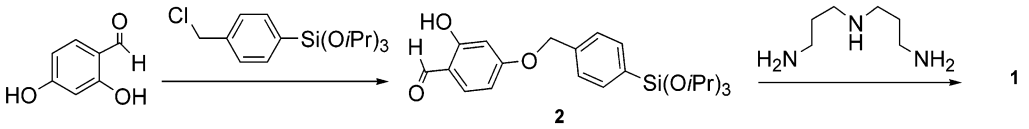

tion). MS (FAB+, NBA): m/z = 1022 ((M + H$^+$), 8), 727 (M−$CH_2PhSi(OiPr)_3$ + H)$^+$, 5). IR (cm^{-1}, KBr): 2976−2932 (ν C_{sp3}−H), 1627 (ν C═N), 1605−1463 (ν C═C), 1038 (ν Si−O). Anal. Calcd for $C_{52}H_{75}N_3O_{10}Si_2Cu$: C, 61.11; H, 7.40; N, 4.11; Si, 5.50; Cu, 6.22. Found: C, 60.97; H, 7.30; N, 3.94; Si, 5.85; Cu, 6.02.

Preparation of Xerogels (Route A). The hydrolysis and polycondensation of **3** and **4** have been carried out according to the same procedure. The preparation of **X3d** is given as an example. For the other xerogels only physical data are given below.

*Preparation of **X3d***. A solution of **3** (1.00 g, 9.83 × 10^{-4} mol) in *i*PrOH (4 mL) was placed in a 20-mL Pyrex test tube under argon. Then 53 μL (2.95 × 10^{-3} mol) of water and 200 μL (1.97 × 10^{-4} mol) of a TBAF solution (1 M) were added at room temperature with a syringe. The solution was stirred and then placed in a thermostated water bath at 30 °C without stirring. After 3 h, a gel was formed. The brown gel was allowed to age for 5 days at 30 °C, after which it was powdered and washed with *i*PrOH, acetone, and ether in a glovebox. The obtained solid was powdered again and dried under vacuum (0.1 Torr) for 12 h at 120 °C, to yield 650 mg of **X3d** as a brown powder. S_{BET} = 20 m^2·g^{-1}. IR (cm^{-1}, KBr): 3400 (ν H-bonded Si−OH), 2958−2920−2850 (ν C_{sp3}−H), 1620 (ν C═N), 1602−1458 (ν C═C), 1150−1000 (ν Si−O−Si). Anal. Calcd for $C_{34}H_{43}N_3O_{12}Si_2Co$: C, 51.00; N, 5.25; Si, 7.00; Co, 7.36. Found: C, 50.71; N, 4.84; Si, 8.20; Co, 6.80.

X3a. S_{BET} < 10 m^2·g^{-1}. IR (cm^{-1}, KBr): 3600 (ν free O−H), 3401−3237 (ν H-bonded O−H), 3052−3020 (ν C_{sp2}−H), 2978−2922−2867 (ν C_{sp3}−H), 1627 (ν C═N), 1600−1458 (ν C═C), 1070 (ν Si−O−Si). Anal. Calcd for $C_{34}H_{33}N_3O_7Si_2Co$, $3H_2O$: C, 53.41; N, 5.49; Si, 7.33; Co, 7.71. Found: C, 54.15; N, 4.93; Si, 8.80; Co, 5.50.

X3b. S_{BET} < 10 m^2·g^{-1}. Anal. Calcd for $C_{34}H_{33}N_3O_7Si_2Co$·$3H_2O$: C, 53.41; N, 5.49; Si, 7.33; Co, 7.71. Found: C, 54.15; N, 5.53; Si, 7.40; Co, 6.70.

X3c. S_{BET} < 10 m^2·g^{-1}. Anal. Calcd for $C_{34}H_{33}N_3O_7Si_2Co$·$3H_2O$: C, 53.41; N, 5.49; Si, 7.33; Co, 7.71. Found: C, 54.42; N, 5.34; Si, 8.80; Co, 6.35.

X3e. S_{BET} = 102 m^2·g^{-1}, V_p = 0.12 cm^3·g^{-1}. Anal. Calcd for $C_{34}H_{33}N_3O_7Si_2Co$·$5H_2O$: C, 51.00; N, 5.25; Si, 7.0 0; Co,7.36. Found: C, 51.46; N, 5.05; Si, 9.32; Co, 6.63.

X3f. S_{BET} = 134 m^2·g^{-1}, V_p = 0.14 cm^3·g^{-1}. Anal. Calcd for $C_{34}H_{33}N_3O_7Si_2Co$·$5H_2O$: C, 51.00; N, 5.25; Si, 7.00; Co, 7.36. Found: C, 50.97; N, 4.99; Si, 11.00; Co, 6.95.

X3g. S_{BET} = 207 m^2·g^{-1}, V_p = 0.21 cm^3·g^{-1}. Anal. Calcd for $C_{34}H_{33}N_3O_7Si_2Co$·$7H_2O$: C, 48.80; N, 5.02; Si, 6.69; Co, 7.05. Found: C, 48.92; N, 4.69; Si, 10.52; Co, 6.62.

X$_9$3e. S_{BET} = 451 m^2·g^{-1}, V_p = 0.61 cm^3·g^{-1}. Anal. Calcd for $C_{34}H_{33}N_3O_{25}Si_{11}Co$·$5H_2O$: C, 30.45; H, 3.20; N, 3.13; Si, 22.98; Co, 4.39. Found: C, 30.16; H, 3.66; N, 2.55; Si, 23.35; Co, 3.10.

X$_{19}$3e. S_{BET} = 479 m^2·g^{-1}, V_p = 0.54 cm^3·g^{-1}. Anal. Calcd for $C_{34}H_{33}N_3O_{45}Si_{21}Co$·$20H_2O$: C, 18.46; H, 3.30; N, 1.90; Si, 26.60; Co, 2.67. Found: C, 24.63; H, 3.31; N, 1.95; Si, 23.90; Co, 2.10.

X4a. S_{BET} < 10 m^2·g^{-1}. RMN ^{29}Si (δ, 60 MHz, CP-MAS): −70 (T^2); −77 (T^3). Anal. Calcd for $C_{34}H_{33}N_3O_7Si_2Cu$·H_2O: C, 55.69; N, 5.73; Si, 7.64; Cu, 8.67. Found: C, 55.56; N, 5.05; Si, 6.60; Cu, 7.82.

X$_9$4h. S_{BET} = 434 m^2·g^{-1}, V_p = 0.59 cm^3·g^{-1}. Anal. Calcd for $C_{34}H_{33}N_3O_{25}Si_{11}Cu$: C, 32.51; N, 3.35; Si, 24.59; Cu, 5.06. Found: C, 32.57; N, 2.80; Si, 20.65; Cu, 3.50.

X$_{19}$4h. S_{BET} = 569 m^2·g^{-1}, V_p = 0.80 cm^3·g^{-1}. Anal. Calcd for $C_{34}H_{33}N_3O_{45}Si_{21}Cu$·$5H_2O$: C, 22.88; H, 2.15; N, 2.10; Si, 29.51; Cu, 3.18. Found: C, 24.69; H, 2.55; N, 2.38; Si, 24.90; Cu, 2.70.

Route B. *Preparation of **X1***. To a solution of **1** (1.72 g, 1.79 mmol) in *i*PrOH (1.8 mL) placed in a flask under argon were added 97 μL of water (5.37 mmol) and 360 μL (3.58 × 10^{-4} mol) of a TBAF solution (1 M) in THF. The flask was then placed in a water bath at 30 °C with stirring. Gelation occurred after 10 min. The wet yellowish gel was allowed to age for 5 days at 30 °C. It was then powdered and washed with *i*PrOH, acetone, and diethyl ether. This treatment was repeated twice and the obtained solid was powdered again and dried for 12 h at 120 °C under 0.05 Torr to yield 1.09 g of xerogel **X1** as a yellow powder. ^{13}C NMR (δ, 75 MHz, CP-MAS): 31.9 (CH_2−CH_2−CH_2), 48.2 (NH−CH_2), 58.0 (C═N−CH_2), 70.2 (OCH_2), 103.6−108.1−113.0−127.6−134.2−139.6 (C_{arom}), 163.5 (C═N). ^{29}Si NMR (δ, 60 MHz, CP-MAS): −71 (T^2), −79 (T^3). S_{BET} = 98 m^2·g^{-1}. IR (cm^{-1}, KBr): 3400 (ν H-bonded Si−OH), 3058−3016 (ν C_{sp2}−H), 2916−2838 (ν C_{sp3}−H), 1622 (ν C═N), 1600−1454 (ν C═C), 1150−1000 (ν Si−O−Si). Anal. Calcd for $C_{34}H_{35}N_3O_7Si_2$: C, 62.46; H, 5.40; N, 6.43; Si, 8.59. Found: C, 62.22; H, 5.30; N, 5.93; Si, 9.40.

*Reactivity of **X1** with Cobalt and Copper Acetylacetonate.* Before reaction, xerogels were dried for 12 h at 120 °C under 0.1 Torr. The quantity of metal salt was calculated considering a complete condensation of the xerogel. Solvents were dried and carefully degassed just before use. Complexations were achieved under an argon atmosphere in *i*PrOH heated under reflux for 24 h. Solids were then washed with *i*PrOH.

The procedure for incorporation of cobalt(II) or copper(II) into **X1** is similar. The preparation of **X1[Co]** is given as an example. Complexation reactions were done under an argon atmosphere to avoid dioxygen and moisture contamination.

*Preparation of **X1[Co]***. A solution of 361 mg (1.41 × 10^{-3} mol) of cobalt acetylacetonate in *i*PrOH (60 mL) was added dropwise to a suspension of **X1** (460 mg, 7.03 × 10^{-4} mol) in *i*PrOH (10 mL). The solid became instantly brown and the solution purple. The reaction mixture was heated under reflux with stirring for 24 h. The solid was filtrated and washed successively with *i*PrOH, acetone, and diethyl ether until the filtrate became colorless. It was then dried at 120 °C under 0.06 Torr to give 620 mg of **X1[Co]** as a brown powder. S_{BET} = 122 m^2·g^{-1}, V_p = 0.30 cm^3·g^{-1}. IR (cm^{-1}, KBr): 3414 (ν H-bonded Si−OH), 3060−3008 (ν C_{sp2}−H), 2916−2852 (ν C_{sp3}−H), 1618 (ν C═N), 1600−1450 (ν C═C), 1150−1000 (ν Si−O−Si). Anal. Calcd for $C_{34}H_{41}N_3O_{11}Si_2Co$: C, 52.18; N, 5.37; Si, 7.16; Co, 7.53. Found: C, 52.30; N, 4.96; Si, 8.89; Co, 6.54.

X1[Cu]. S_{BET} = 118 m^2·g^{-1}, V_p = 0.28 cm^3·g^{-1}. IR (cm^{-1}, KBr): 3410 (ν H-bonded Si−OH), 3054 (ν C_{sp2}−H), 2970−2882 (ν C_{sp3}−H), 1626 (ν C═N), 1602−1464 (ν C═C), 1150−1000 (ν Si−O−Si). Anal. Calcd for $C_{34}H_{39}N_3O_{10}Si_2Cu$: C, 53.08; N, 5.46; Si, 7.28; Co, 8.26. Found: C, 53.52; N, 5.01; Si, 9.03; Cu, 7.82.

Results and Discussion

The bis-silylated Schiff base **1** was prepared according to the way depicted in Scheme 2: the 2,4-dihydroxybenzaldehyde was first regioselectively silylated in the para position[28] to afford **2**, which was subsequently condensed with 3,3′-diaminodipropylamine to give **1**. The structural characterization of **1** was based on NMR spectroscopy and elemental analyses. Metal Schiff base complexes **3** and **4** were achieved in high yield by exchange reaction between the appropriate dried metal acetylacetonate salts and the Schiff base **1** (Scheme 1). They were characterized by elemental analyses. It is

(28) Mendelson, W. L.; Holmes, M.; Dougherty, J. *Synth. Commun.* **1996**, *26*, 593−601.

Table 1. Infrared Data (cm^{-1}) for Different Samples

sample	**1**	**3**	**X1**	**X3d**	**4**	**X_{19}4h**
$\nu_{C=N}$	1627	1627	1622	1620	1627	1627

worth noting that the infrared spectra of complexes **3** and **4** display a $\nu_{C=N}$ stretching band very close to that of the corresponding ligand (see Table 1 and Experimental Section). That strongly suggests the pentacoordination of the complexes **3** and **4**. Indeed, Taylor et al. have observed a weak difference (0−10 cm^{-1}) between the $\nu_{C=N}$ stretching band of a Schiff base and the corresponding five-coordinate Co(II) Schiff base complex whereas a 35-cm^{-1} shift was observed in the case of the formation of four-coordinate complexes.[29]

Preparation of Xerogels According to Route A. The hydrolytic polycondensation of **3** and **4** was performed in the presence of a stoichiometric amount of water (3 equiv) and tetrabutylammonium fluoride (TBAF) as catalyst. In all cases, the gelations were achieved under an argon atmosphere. The gelation of the cobalt(II) Schiff base complex **3** was performed under different experimental conditions, which are reported in Table 2. Gelation of **4** was carried out in THF only, due to the insolubility of **4** in 2-propanol. Cohydrolysis and polycondensation of **3** and **4** with 9 or 19 equiv of tetraisopropyl orthosilicate (Si(O*i*Pr)$_4$) was also carried out to study the influence of the dilution of organic units into silica on the dioxygen uptake of the corresponding materials. Monolithic gels or co-gels were obtained within 30 min. They were allowed to age for 5 days at the temperature of the gelation. Then, they were washed under an argon atmosphere with the reaction solvent, acetone, and ether. Finally, the powders were dried (120 °C for 12 h under 0.06 Torr) to afford the xerogels **X*ny*** (***n*** being the number of the precursor and ***y*** a letter specifying the experimental conditions of the gelation indicated in Table 2). The co-gels are named **X$_z$*ny***, the index ***z*** indicating the number of equivalents of Si(O*i*Pr)$_4$.

Despite the presence of Co(II) or Cu(II), ^{29}Si NMR spectra of some **X*ny*** materials have been recorded and they display a major resonance centered at $\delta = -76$ ppm (T^3 substructures) as well as another at −70 ppm (T^2 substructures). The absence of signals between −90 and −110 ppm denotes that there was no Si−C bond cleavage during the sol−gel process.

The BET surface areas of the xerogels were determined by N_2 adsorption−desorption measurements and the average pore diameters by the BJH method.[27] Results are reported in Table 2. They show that the materials prepared at 30 °C in the presence of 10% TBAF have low surface areas, whatever the solvent and the precursor (entries 1−4 and 10, Table 2). It is worth noting that the SEM images of **X3d** and **X3a** revealed that the average particle size for **X3d** is about 10 μm while it is about 300 μm for **X3a**. Thus, the granulometry of materials with low surfaces areas prepared from the precursor **3** is highly dependent on the solvent used for the gelation.

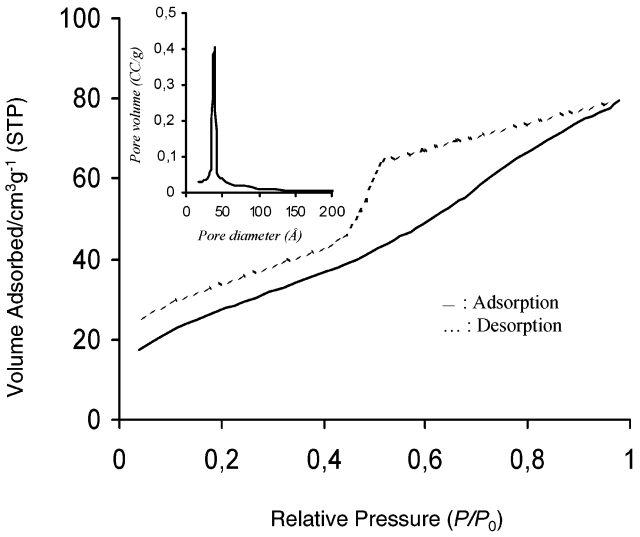

Figure 2. Nitrogen adsorption−desorption isotherm and pore size distribution plot (inset) of **X3e**.

The texture of **X*ny*** materials is not highly dependent on the amount of catalyst (entries 5 and 6, Table 2) (TBAF 1 or 10%). In contrast, the specific surface areas increase as a function of the temperature (entries 4 and 5, Table 2). Furthermore, the N_2 adsorption−desorption isotherms for the materials prepared at 80 °C (entries 5, 6, and 7, Table 2) are of type IV, characteristic of mesoporous materials with a rather narrow pore size distribution (Figure 2). The contribution of micropores to the texture of **X3e** was very low and the hysteresis is not closed due to the presence of pores with ink-bottle shape and small pore openings that do not facilitate the nitrogen desorption.

The FTIR spectra of the materials containing Co(II) or Cu(II) Schiff base complexes exhibit the C═N stretch-

Table 2. Textural Characteristics of Materials Prepared from 3 and 4 in the Presence of TBAF 10%

entry	solvent	precursor	[M][a] (mol L^{-1})	*T* (°C)	material designation	S_{BET} ($m^2 \cdot g^{-1}$)	pore vol ($cm^3 \cdot g^{-1}$)	Dp[b] (Å)
1	THF	**3**	0.5	30	**X3a**	<10		
2	CH_2Cl_2	**3**	1	30	**X3b**	<10		
3	CH_2Cl_2[c]	**3**	1	30	**X3c**	<10		
4	*i*PrOH	**3**	0.2	30	**X3d**	20		
5	*i*PrOH	**3**	0.2	80	**X3e**	102	0.12	30−50
6	*i*PrOH	**3**	0.2	80	**X3f**[d]	134	0.14	30−50
7	*i*PrOH	**3**	0.2	80	**X3g**[d,e]	207	0.21	30−50
8	*i*PrOH	**3**	1	80	**$X_9$3e**[f]	451	0.61	<20, >50
9	*i*PrOH	**3**	1	80	**X_{19}3e**[g]	479	0.54	<30, >90
10	THF	**4**	0.5	30	**X4a**	<10		
11	THF	**4**	1	65	**$X_9$4h**[f]	434	0.59	>30
12	THF	**4**	1	65	**X_{19}4h**[g]	569	0.81	>50

[a] Concentration in precursor. [b] Calculated from the desorption branch of the N_2 isotherm by using the BJH method. [c] Hydrolytic polycondensation under an air atmosphere. [d] TBAF 1%. [e] Sealed tube. [f] Co-gel with 9 equiv of (*i*PrO)$_4$Si. [g] Co-gel with 19 equiv of (*i*PrO)$_4$Si.

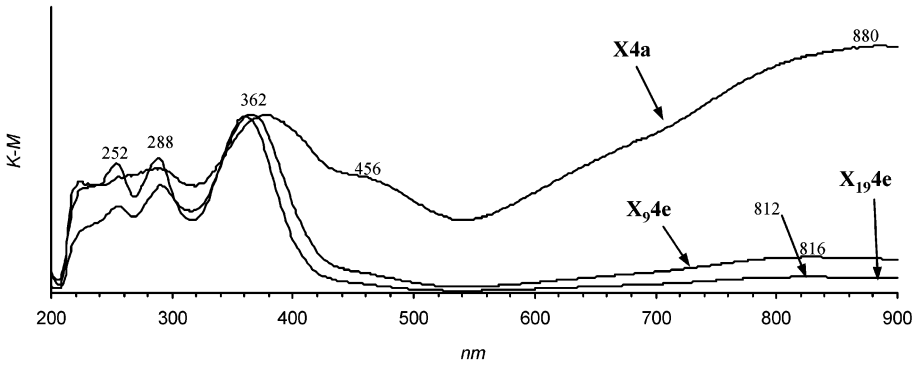

Figure 3. Solid state diffuse reflectance spectra of **X4a**, **X$_9$4e**, and **X$_{19}$4e**.

ing vibration at a frequency very close to that for the corresponding molecular precursor (Table 1). That means that only small changes in metal−ligand geometry took place during the gelation and the pentacoordination of complexes survives the sol−gel process.

Materials have also been prepared from the copper complex **4**. The remarks concerning the textural data, which depend on the experimental conditions, are similar to those done from **3** (Table 2).

The electronic spectra for various materials containing metal Schiff base complexes were recorded to provide insight into complexes geometry within the solids. This study was performed on materials containing Cu(II) complexes. The diffuse reflectance spectra of **X4a**, **X$_9$4e**, and **X$_{19}$4e** are reported in Figure 3. The bands in the vicinity of 360−380 nm were attributed to d−π* charge transfer between Cu(II) and Schiff base. The absence of bands around 640 nm excludes a square planar tetracoordinated geometry cis-N_2O_2 around the metal.[30] The broad bands centered respectively at 880 nm for **X4a**, 816 for **X$_9$4e**, and 812 for **X$_{19}$4e** are attributed to d−d transitions. They most probably denote a pentacoordination around the metal with a geometry corresponding to a distorded trigonal bipyramid.[31−33] It is worth noting that a blue shift of the d−d transitions as well as a decrease of the intensity of this transition were observed with the dilution of the complexes within silica matrix (Figure 3), the spectra having been standardized on the d−π* charge-transfer band at 360−380 nm.

Preparation and Characterization of the Hybrid Material Obtained from 1. The hydrolytic polycondensation of a 1 M 2-propanol solution of **1** was performed at 30 °C in the presence of a stoichiometric amount of H_2O and 10 mol % of TBAF as catalyst, under an argon atmosphere. The gel, which was obtained after about 10 min, underwent the workup described in the preceding paragraph, giving rise to xerogel **X1**.

The solid state ^{29}Si NMR spectrum of **X1** displayed a major resonance at −79 ppm attributed to the T^3 substructure, indicating a very well condensed solid.

Table 3. Some Relevant Textural Data for X1, X1[Cu], and X1[Co]

sample	[M][a] (mmol·g^{-1})	% of complexed moieties	S_{BET} (m^2·g^{-1})	V_t[b] (cm^3·g^{-1})	Dp[c] (Å)	V_p[d] (cm^3·g^{-1})
X1	0	0	98	0.25	50−150	0.24
X1[Cu]	1.23	103	118	0.28	80−150	0.28
X1[Co]	1.11	94	122	0.30	70−150	0.29

[a] Concentration in metal calculated from elemental analysis. [b] V_t, total pore volume. [c] Calculated from the desorption branch of the N_2 isotherm by using the BJH method. [d] Calculated at the desorption.

The absence of resonance corresponding to Q substructures (region near −100 ppm) shows that no cleavage of Si−C bond occurred during the sol−gel process. The solid state ^{13}C NMR spectrum of **X1** revealed that the organic moieties are intact within the material, the chemical shifts being the same as those observed in solution for **1** (see Experimental Section). The FTIR spectrum of **X1** displays a band at 1622 cm^{-1} attributed to the C═N stretching vibration of the imino group.[34] The BET surface area of the **X1** was found to be 98 m^2 g^{-1} (Table 3).

Study of the Complexing Properties of X1 (Route B). Complexation of the Schiff bases incorporated within **X1** was achieved by treatment of the material with a 2-propanol solution containing an excess of copper(II) or cobalt(II) acetylacetonate at reflux for 24 h under an argon atmosphere. The solids were filtered and washed with 2-propanol, acetone, and ether under an argon atmosphere, until the filtrate became colorless to give respectively **X1[Cu]** and **X1[Co]**. The percentage of complexed sites was inferred from the results of the elemental analysis of the metal and nitrogen. The results reported in Table 3 show that the complexation was almost quantitative.

The N_2 adsorption−desorption isotherms for **X1[Cu]** and **X1[Co]** are very similar to that of the starting material **X1**. They are of type IV, characteristic of mesoporous materials with a broad pore size distribution centered at 100 Å.

The FTIR spectrum for **X1[Cu]** and **X1[Co]** displayed a $\nu_{C=N}$ stretching vibration at 1626 and 1618 cm^{-1}, respectively, whereas the C═N stretching vibration of **X1** was at 1622 cm^{-1}. These low shifts suggest also a pentacoordination[29] of the metal as it was previously observed for the materials **X3** and **X4**.

(29) Niswander, R. H.; Taylor, L. T. *Inorg. Chem.* **1976**, *15*, 2360−2364.
(30) Tidjani-Rahmouni, N.; Djebbar-Sid, S.; Chenah, N.; Benali-Baitich, O. *Synth. React. Inorg. Met.-Org. Chem.* **1999**, *29*, 979−994.
(31) Hathaway, B. J.; Dudley, R. J.; Nicholls, P. *J. Chem. Soc. A* **1969**, 1845−1848.
(32) Hathaway, B. J.; Procter, I. M.; Slade, R. C.; Tomlinson, A. A. G. *J. Chem. Soc. A* **1969**, 2219−2224.
(33) Boca, R.; Elias, H.; Haase, W.; Huber, M.; Klement, R.; Muller, L.; Paulus, H.; Svoboda, I.; Valko, M. *Inorg. Chim. Acta* **1998**, *278*, 127−135.
(34) Heinert, D.; Martell, A. E. *J. Am. Chem. Soc.* **1962**, *84*, 3257−3263.

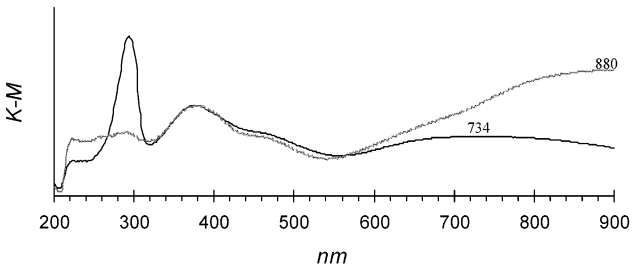

Figure 4. Solid state diffuse reflectance spectra of **X3a** (gray line) and **X1**[**Cu**] (dark line).

To have more information concerning the geometry around the metal in the Schiff base complexes within the materials, a UV−visible study for **X1[Cu]** was done. The diffuse reflectance spectrum displays an intense $\pi-\pi^*$ band at 292 nm and a d−π^* band at 370 nm. These bands are respectively characteristic of aromatic groups and charge transfer between Cu(II) and the Schiff base ligand. The spectrum of **X1[Cu]** exhibits also a shoulder at 450 nm and a broad band at 734 nm, associated with d−d transitions. These values exclude the tetracoordination of the Cu(II)[30] and suggest a geometry intermediate between a square planar pyramid and a trigonal bipyramid.[35,36] Indeed, the UV−visible literature data in relation to crystallographic data associate a square planar pyramid with an absorption band in the vicinity of 550−670 nm whereas a trigonal bipyramid displays a band in the vicinity of 800−850 nm.[31,32]

Comparison between Routes A and B. The comparison of the UV−visible spectra of **X3a** (Figure 4, Route A) and **X1[Cu]** (Figure 4, Route B) points out some differences denoting that both routes leading to materials containing metal Schiff base complexes are not equivalent. For example, the d−d transition is at 880 nm for **X3a** while it is at 734 nm for **X1[Cu]**. We consider that the geometry around the metal center within **X3a** corresponds to a distorted trigonal bipyramid while the geometry around the metal center within **X1[Cu]** is between a planar square pyramid and a trigonal bipyramid. Indeed, the geometry of **3** is probably maintained during the sol−gel process (route A). In contrast, the formation of immobilized Schiff base complexes according to route B involves the metal adopting the geometry of the immobilized Schiff base. As the Schiff base is flexible, it should undergo significant distortions during the sol−gel process, which explains that in this case the geometry around the metal center is most probably between a trigonal bipyramid and a square pyramid.

Dioxygen Adsorption on Hybrid Materials Containing Co(II) Schiff Base Complexes. The capacity of hybrid materials containing Co(II) Schiff bases covalently linked to the silica matrix by two Si−C bonds was evaluated by static volumetric gas uptake measurements at room temperature. The results are reported in Tables 4−6.

The dioxygen sorption for the materials **X3d** (1st cycle) is shown in Figure 5 and compared to nitrogen sorption, which can be considered as a blank due to nonselective adsorption of gas on the material. As we have previously shown,[20,37] the equilibrium constant for dioxygen binding, K_{O2}, was calculated using a double adsorption process[38,39] derived by analogy with the multiple-site Langmuir-type adsorption model to take into account both the chemisorption of dioxygen on cobalt complexes and the nonselective adsorption onto the silica matrix.

Table 4. Thermodynamic Data at 293 K for Dioxygen and Nitrogen Adsorption by X3d and X1[Co][a]

sample	cycle	V_{O2}[b] ($cm^3 \cdot g^{-1}$)	V_{N2}[b] ($cm^3 \cdot g^{-1}$)	$(P_{O2})_{1/2}$[c,d] (Torr)	% of active sites[e]
X3d	1	11.0	0.4	9.7	41
	2	7.9		19	29
	3	8.0		15.6	29
X1[Co]	1	3.5	1.3	4.7	9
	2	3.0		3.1	7

[a] Materials treated before reaction with dioxygen and for each recycling experiment at 120 °C under 10^{-3} Torr for 6−12 h. [b] Volume adsorbed at 760 Torr. [c] Determined from the Langmuir isotherm (see text). [d] $(P_{O2})_{1/2} = 1/K_1$. [e] Assuming a 1:1 complex (O_2:Co).

Table 5. Thermodynamic Data at 293 K for Dioxygen and Nitrogen Adsorption by Materials X3g

entry	cycle	V_{O2}[c] ($cm^3 \cdot g^{-1}$)	V_{N2}[c] ($cm^3 \cdot g^{-1}$)	$(P_{O2})_{1/2}$[d,e] (Torr)	% of active sites[f]
1	1[a]	4.4	0.3	33.5	17
2	2[a]	2.9		37.2	11
3	3[a]	4.4		34.5	17
4	4[a]	1.6		20.5	5
5	1[b]	6.2	0.3	48.6	25
6	2[b]	7.8		28.2	31
7	3[b]	6.8		44.5	27

[a] Treatment before reaction at 20 °C under 10^{-3} Torr for 12 h. [b] Treatment before reaction at 120 °C under 10^{-3} Torr for 12 h. [c] Volume adsorbed at 760 Torr. [d] Determined from the Langmuir isotherm (see text). [e] $(P_{O2})_{1/2} = 1/K_1$. [f] Assuming a 1:1 complex (O_2:Co).

The results reported in Table 4 show that the material **X3d** prepared according to route A (i.e., gelation of the base Schiff complex) has a better oxygen binding capacity than **X1[Co]** prepared according to route B.

The dioxygen sorption of the material **X3g** was studied after treatment at 20 °C under 10^{-3} Torr and after treatment at 120 °C under the same pressure (Table 5). The results show that the dioxygen uptake on **X3g** is higher at 120 °C (entries 5−7) than at 20 °C (entries 1−4). Therefore, we treated all the materials at 120 °C under 10^{-3} Torr before reaction.

The results reported in Table 6 clearly show that the surface area of the solids is not a dominating factor for dioxygen uptake, as the mesoporous materials **X3e**−**g** (entries 5−7) with a rather narrow pore size distribution are not more reactive toward dioxygen than the nonporous materials **X3a** and **X3d** (entries 1 and 4). Furthermore, the dioxygen sorption for the nonporous solids **X3a**−**d** (entries 1−4) is very different, which should be due to a different granulometry of these materials. Indeed, we have previously noted that the

(35) Boge, E. M.; Freyberg, D. P.; Kokot, E.; Mockler, G. M.; Sinn, E. *Inorg. Chem.* **1977**, *16*, 1655−1660.
(36) Kolis, J. W.; Hamilton, D. E.; Kildahl, N. K. *Inorg. Chem.* **1979**, *18*, 1826−1831.
(37) Dubois, G.; Tripier, R.; Brandès, S.; Denat, F.; Guilard, R. *J. Mater. Chem.* **2002**, *12*, 2255−2261.
(38) Drago, R. S.; Webster, C. E.; McGilvray, J. M. *J. Am. Chem. Soc.* **1998**, *120*, 538−547.
(39) Webster, C. E.; Cottone, A., III; Drago, R. S. *J. Am. Chem. Soc.* **1999**, *121*, 12127−12139.

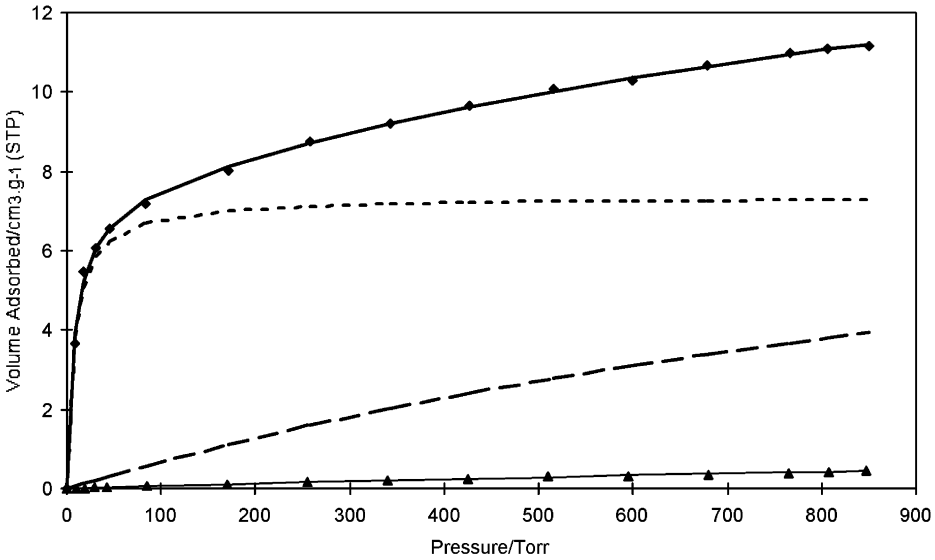

Figure 5. Adsorption isotherm of ◆ O_2 and ▲ N_2 by **X3d** at 293 K, with calculated isotherm for O_2, --- component 1 of the isotherm (chemisorption), – – – component 2 of the isotherm (nonselective adsorption).

Table 6. Thermodynamic Data at 293 K for Dioxygen and Nitrogen Adsorption by Materials Containing Co(II) Schiff Base Complexes[a]

entry	sample	S_{BET} ($m^2 \cdot g^{-1}$)	cycle	V_{O2}[b] ($cm^3 \cdot g^{-1}$)	V_{N2}[b] ($cm^3 \cdot g^{-1}$)	$(P_{O2})_{1/2}$[c,d] (Torr)	% of active sites[e]
1	**X3a**	<10	1	6.2	0.6	19.6	30
			2	4.8		19.7	23
			3	4.5		19.6	21
2	**X3b**	<10	1	2.7	0.1	5.6	10
			2	1.2		30.5	4
			3	1.6		29.7	6
3	**X3c**	<10	1	2.3	0.2	3.3	9
			2	2.2		10.3	8
			3	2.9		5.1	11
4	**X3d**	20	1	11.0	0.4	9.7	41
			2	7.9		19.0	29
			3	8.0		15.6	29
5	**X3e**	102	1	10.0		10.6	37
			2	8.1		10.1	29
			3	6.2	0.8	11.3	22
6	**X3f**	134	1	9.2		3.4	31
			2	8.2		7.9	27
			3	8.1	1.0	5.8	27
7	**X3g**	207	1	6.2	0.3	48.6	25
			2	7.8		28.2	31
			3	6.8		44.5	27
8	**$X_9$3e**	451	1	4.5	0.8	7.1	38
			2	2.4		4.5	14
			3	3.6		4.5	24
			4	2.9		5.7	18
9	**X_{19}3e**	479	1	2.3	0.4	5.3	23
			2	1.7		11.4	16
			3	1.3		4.7	11

[a] Materials treated before reaction with dioxygen and for each recycling experiment at 120 °C under 10^{-3} Torr for 6–12 h. [b] Volume adsorbed at 760 Torr. [c] Determined from the Langmuir isotherm (see text). [d] $(P_{O2})_{1/2} = 1/K_1$. [e] Assuming a 1:1 complex (O_2:Co).

solid **X3a** prepared in THF (entry 1, Table 2) as well as the solids **X3b** and **X3c** prepared in CH_2Cl_2 (entries 2 and 3, Table 2) appear as a solid block with a granulometry around 300 μm while the solid **X3d** prepared in 2-propanol is a fine powder. The diffusion of dioxygen through the fine powder of **X3d** is probably easier than that through the solid block, which could explain the better ability for dioxygen uptake of **X3d** in comparison to that of **X3a**–**c**.

The thermodynamic data show that these materials incorporating Co(II) Schiff base complexes exhibit a great affinity toward dioxygen with $(P_{O2})_{1/2}$ (= $1/K_1$) varying from 3 to 48 Torr depending on the condition of preparation of the xerogels. The total V_{O2} adsorbed at 760 Torr ranges from 2.3 to 11 $cm^3 \cdot g^{-1}$ in the first cycle, the material **X3d** having the best dioxygen binding capacity among the materials prepared. Indeed, the sorption of **X3d** corresponds to 41% of active species, assuming a 1:1 (O_2:Co) dioxygen adduct with a dioxygen uptake equal to 11 $cm^3 \cdot g^{-1}$ and an affinity toward dioxygen, $(P_{O2})_{1/2}$, varying from 8 to 15 Torr. If we compare the adsorption properties of the xerogels described in this paper, to these of cobalt(II) cyanide,[49] cobalt(II) Schiff base,[23,46–48] $[Co(bpy)(tpy)]^{2+}$,[50] $[Co(cyclam)]^{2+}$ [51] complexes incorporated inside zeolite Y, $[Co(cyclam)]^{2+}$ grafted onto silica gel,[37] and Co(salen) incorporated in organic polymers,[15] we can conclude that our materials are among the most effective ones for dioxygen sorption at room temperature, taking into account both the affinity and the capacity toward dioxygen binding.

The study of the dioxygen sorption reversibility shows that the active species in **X3d** appears to be fairly stable after three adsorption/desorption cycles at 120 °C for 6

(40) Vaska, L. *Acc. Chem. Res.* **1976**, *9*, 175–183.
(41) Smith, T. D.; Pilbrow, J. R. *Coord. Chem. Rev.* **1981**, *39*, 295–383.
(42) Tovrog, B. S.; Drago, R. S. *J. Am. Chem. Soc.* **1974**, *96*, 6765–6766.
(43) Niswander, R. H.; Taylor, L. T. *J. Am. Chem. Soc.* **1977**, *99*, 5935–5939.
(44) Niswander, R. H.; Taylor, L. T. *J. Magn. Reson.* **1977**, *26*, 491–503.
(45) Diaz, J. F.; Balkus, K. J.; Bedioui, F.; Kurshev, V.; Kevan, L. *Chem. Mater.* **1997**, *9*, 61–67.
(46) Herron, N. *Inorg. Chem.* **1986**, *25*, 4714–4717.
(47) De Vos, D. E.; Feijen, E. J. P.; Schoonheydt, R. A.; Jacobs, P. A. *J. Am. Chem. Soc.* **1994**, *116*, 4746–4752.
(48) De Vos, D. E.; Thibault-Starzyk, F.; Jacobs, P. A. *Angew. Chem., Int. Ed. Engl.* **1994**, *33*, 431–433.
(49) Taylor, R. J.; Drago, R. S.; Hage, J. P. *Inorg. Chem.* **1992**, *31*, 253–258.
(50) Imamura, S.; Lunsford, J. H. *Langmuir* **1985**, *1*, 326–330.
(51) De Vos, D. E.; Vanoppen, D. L.; Li, X. Y.; Libbrecht, S.; Bruynseraede, Y.; Knops-Gerrits, P. P.; Jacobs, P. A. *Angew. Chem., Int. Ed. Engl.* **1995**, *34*, 144–149.

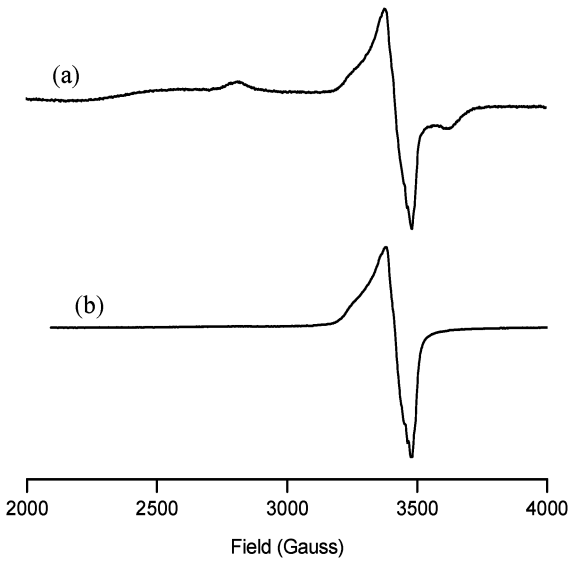

Figure 6. ESR spectra recorded at 100 K for (a) **X3d** and (b) **$X_9$3e** xerogels after exposure to dioxygen.

h under 10^{-3} Torr, 72% of the Co(II) complexes still being active after three cycles.

To have some information concerning the coordination mode on the cobalt center,[7,8,22,40,41] the ESR spectra were recorded at 100 K for the xerogels **X3**. Under anaerobic conditions, a signal of weak intensity, typical of a superoxide species, was observed, probably due to diffusion of a small amount of dioxygen into the ESR sample. The absence or the very low intensity of the Co(II) ESR spectrum near $g = 2.6$ before and after exposure of the materials to dioxygen (Figure 6a) indicates that the active sites are probably silent at 100 K. This suggests that the complex is mainly in a high-spin state ($S = {}^3/_2$), as already mentioned for other tetra- and pentacoordinated Schiff bases Co(II) complexes[33,42−45] incorporated into zeolite Y.[46−48] After exposure to dioxygen, a symmetrical signal at $g \approx 2$ was observed for all the xerogels, as shown in Figure 6b for **$X_9$3e**, which is typical of a superoxide radical. The hyperfine splitting $A_{\parallel}^{Co}$, due to coupling between the radical and the nuclear spin $I_{Co} = {}^7/_2$, is not observed. It is certainly due either to a high concentration of metal center inducing some spin−spin interactions between radicals broadening the signal or/and a lower homogeneity in the solids compared to a solution of superoxide species.

Finally, the dioxygen binding capacity for cogels **$X_9$3e** and **X_{19}3e** (entries 8 and 9, Table 6) in which the Co(II) Schiff base complexes are diluted into the matrix was investigated. The results show that the dilution of the organic moieties induces a decrease of the dioxygen uptake in comparison to the results obtained for the pure material **X3e**. However, the percentage of active sites is still rather high, taking into account the distance of cobalt centers from each other.

Thus, these last results in addition to the ESR data and volumetric measurements suggest that the active species might be a mononuclear superoxidic dioxygen adduct.

Conclusions

In this paper, two routes leading to hybrid materials containing metal Schiff base complexes covalently bonded to the silica matrix by two Si−C bonds were investigated using the sol−gel process. The first corresponds to the hydrolysis and polycondensation of a bis-silylated metal Schiff base complex (route A). This route leads to complexes with trigonal bipyramidal geometry. The second consists of the hydrolysis and polycondensation of a bis-silylated Schiff base followed by the complexation of organic moieties immobilized on silica (route B). In this case, the geometry around the metal centers is between a square planar pyramid and a trigonal bipyramid. Only the materials prepared according to route A are efficient for dioxygen sorption. This is probably due to the difference of geometry around the metal centers in both materials. The high affinity and capacity toward dioxygen of materials prepared according to route A points out the interest of this approach that requires the synthesis of a bis-silylated Schiff base.

CM0302330